PHYSICAL REVIEW B **70**, 161313(R) (2004)

# Control of electron-spin coherence using Landau level quantization in a two-dimensional electron gas

V. Sih,[1] W. H. Lau,[1] R. C. Myers,[1] A. C. Gossard,[1] M. E. Flatté,[2] and D. D. Awschalom[1,*]
[1]*Center for Spintronics and Quantum Information, University of California, Santa Barbara, California 93106, USA*
[2]*Department of Physics and Astronomy, University of Iowa, Iowa City, Iowa 52242, USA*
(Received 23 July 2004; published 28 October 2004)

Time-resolved optical measurements of electron-spin dynamics in modulation-doped InGaAs quantum wells are used to explore electron spin coherence times and spin precession frequencies in a regime where an out-of-plane magnetic field quantizes the states of a two-dimensional electron gas into Landau levels. Oscillatory features in the transverse spin coherence time and effective $g$ factor as a function of the applied magnetic field exhibit a correspondence with Shubnikov–de Haas oscillations, illustrating a coupling between spin and orbital eigenstates. We present a theoretical model in which inhomogeneous dephasing due to the population of different Landau levels limits the spin coherence time and captures the essential experimental results.

DOI: 10.1103/PhysRevB.70.161313 PACS number(s): 72.25.Rb, 72.25.Dc, 71.70.Ej, 78.47.+p

Electron spins in semiconductors have the potential to form the basis of emerging spintronics[1] and quantum information processing technologies.[2] While the dynamics of both the electron spin and its orbital degree of freedom in a two-dimensional electron gas are well understood, intricate phenomena may be expected in the presence of spin-orbit interactions. Here, we present time-resolved optical measurements of the transverse spin relaxation time $T_2^*$ and effective $g$ factor $g^*$ on two-dimensional electron gases (2DEG) in a set of single InGaAs quantum wells (QW). Both $T_2^*$ and $g^*$ exhibit oscillations when measured as a function of the applied magnetic field that correspond to features in the magnetoresistance, indicating a sensitivity to the Landau-level filling.

An electron in a magnetic field $B$ has a spin precession frequency $\Omega_L = g^* \mu_B B/\hbar$, where $\mu_B$ is the Bohr magneton and $\hbar$ is Planck's constant $h$ divided by $2\pi$. $g^*$ can deviate significantly from the free electron value $g \sim 2.0$ due to spin-orbit coupling. Under the application of a strong out-of-plane magnetic field, the energy spectrum of a 2DEG becomes quantized into Landau levels, in which the trajectory of the electrons can be characterized as a cyclotron orbit with radius $R_c = \sqrt{\hbar/eB}$, where $e$ is the charge of an electron. When $B = B_n = hn_{2D}/en$, where $n_{2D}$ is the sheet density and $n$ is an integer indicating the Landau-level index, there are $n$ filled Landau levels. The spacing between Landau levels is periodic in the reciprocal field, and changing the applied magnetic field changes the filling factor of occupied Landau levels $\nu = hn_{2D}/eB$.

Previous measurements of the electron $g$ factor in a 2DEG as a function of Landau-level filling have been performed primarily using electrically detected electron-spin resonance (EDESR), which records a resonant change in the magnetoresistivity due to an applied microwave excitation.[3,4] The low number of electron spins in a 2DEG makes the direct detection of microwave absorption for conventional ESR difficult.[5] Although EDESR studies have yielded a relation between $g^*$ and $n$, the resonance feature was only observable in a small range of magnetic field where the Fermi energy is located between spin-split Landau levels,[3] and the linewidth measured through the conductivity is not directly related to the spin coherence time.[4] The electron $g$ factor has also been measured using the coincidence method,[6] but these transport measurements can be dominated by exchange interaction.[4] Here, we measure the spin dynamics of optically injected electrons using time-resolved Faraday rotation. This allows us to determine $T_2^*$ and $g^*$ over a wider range of magnetic fields and observe oscillations that indicate a dependence on $\nu$.

Electron-spin coherence and transport measurements are performed on a set of single modulation-doped $In_{0.2}Ga_{0.8}As/GaAs$ QW grown by molecular beam epitaxy. The sample structure is a 50 nm GaAs/30 nm $n$-doped GaAs/20 nm GaAs/7.5 nm $In_{0.2}Ga_{0.8}As$/20 nm GaAs/10 nm $n$-doped GaAs/(001) semi-insulating GaAs substrate. The doping densities of the Si-doped layers are $5\times10^{16}$ $cm^{-3}$ (sample A); $1\times10^{17}$ $cm^{-3}$ (sample B); $3\times10^{17}$ $cm^{-3}$ (sample C); $5\times10^{17}$ $cm^{-3}$ (sample D); and $8\times10^{17}$ $cm^{-3}$ (sample E). Since the absorption energies of these quantum wells (photoluminescence peak at 1.33 eV at temperature $T=5$ K) are lower in energy than the band gap of the GaAs substrate, we can selectively optically excite and detect electron-spin polarization in the quantum well. Low-temperature transport measurements are performed on samples C, D, and E in a magneto-optical cryostat with magnetic fields up to $B=7$ T and reveal clear signatures of Shubnikov–de Haas oscillations. The samples are patterned with a standard 4:1 Hall bar geometry and are measured using lock-in detection with an excitation current of 99 nA at 11 Hz. The electron sheet densities and mobilities at $T=5$ K are $5.4\times10^{11}$ $cm^2$ and $3.8\times10^4$ $cm^2/V$ s (sample C), $6.6\times10^{11}$ $cm^{-2}$ and $3.1\times10^4$ $cm^2/V$ s (sample D), and $7.0\times10^{11}$ $cm^{-2}$ and $2.4\times10^4$ $cm^2/V$ s (sample E). We determine that the electron effective mass in sample E is $0.064m_e$ by fitting the temperature dependence of the amplitudes of the Shubnikov–de Haas oscillations.[7] Optical measurements (spot diameter $\sim 50$ $\mu$m) performed on patterned Hall bar structures (mesa width $\sim 150$ $\mu$m) are found to reproduce the results of unprocessed samples, indicating that the processing has little effect on the electron-spin dynamics of the 2DEG.

 

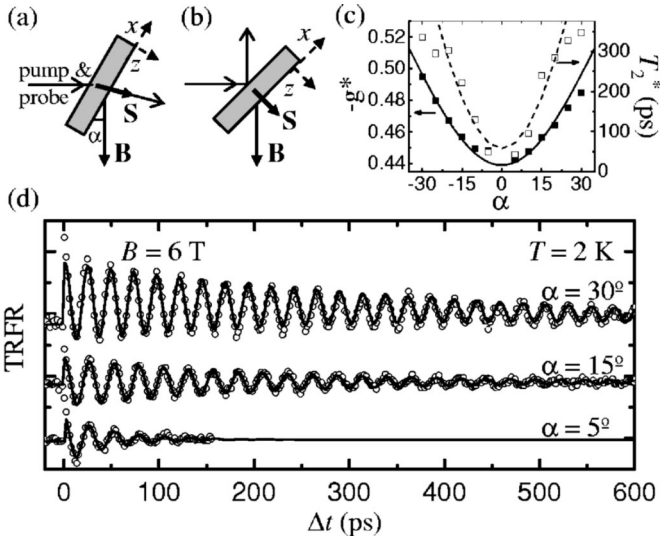


FIG. 1. (a) Transmission and (b) 45° reflection measurement geometries. (c) Effective $g$ factor $g^*$ (■) and spin coherence time $T_2^*$ (□) as a function of angle $\alpha$ at $B=6$ T and $T=2$ K on sample E. The solid curve is a fit to Eq. (2). The dotted line is calculated using Eq. (5). (d) Faraday rotation as a function of the time delay $\Delta t$ on sample E at $\alpha=5°$, 15°, and 30° for $B=6$ T and $T=2$ K.

TRFR, an optical pump-probe spectroscopy, is used to probe the electron-spin dynamics. Using a balanced photodiode bridge and lock-in detection, rotation angles on the order of 10 $\mu$rad can be measured with subpicosecond temporal resolution.[8] The electron-spin magnetization precesses in the plane perpendicular to the applied magnetic field, and the Faraday rotation angle as a function of time delay $\Delta t$ can be expressed as

$$\theta_F(\Delta t) = A_1 e^{-\Delta t/T_1} + A_2 e^{-\Delta t/T_2^*} \cos \Omega_L \Delta t \qquad (1)$$

where $A_1$ ($A_2$) is the amplitude of the electron-spin polarization injected that is parallel (perpendicular) to the magnetic field and $T_1$ is the longitudinal spin coherence time. Although the sign of $g^*$ cannot be determined from such fits, measurements of $In_xGa_{1-x}As$ for $0<x<0.1$ (Ref. 9) and InAs (Ref. 10) indicate that $g^*$ is negative.

Two geometries employed in this measurement are illustrated in Fig. 1: a transmission geometry in which the [110] direction ($x$) can be rotated up to ±30° from the direction of the applied magnetic field by an angle $\alpha$ [Fig. 1(a)] and a reflection geometry where the sample is 45° with respect to the applied field and the optical paths [Fig. 1(b)]. In the latter case, the collection path forms a right angle with the incident light. The sample is mounted so that the magnetic field is in the $(x,z)$ plane. Figure 1(d) shows TRFR measurements at 6 T and 2 K on sample E. A summary of the angle dependence of $T_2^*$ and $g^*$ is plotted in Fig. 1(c). $T_2^*$ increases dramatically with increasing $\alpha$ and out-of-plane magnetic field; this is related to a suppression of the dominant spin relaxation mechanism, which is discussed later in the text.

$g^*$ as a function of $\alpha$ can be fit to determine the components of the $g$ tensor along the $x$ and $z$ directions,[11]

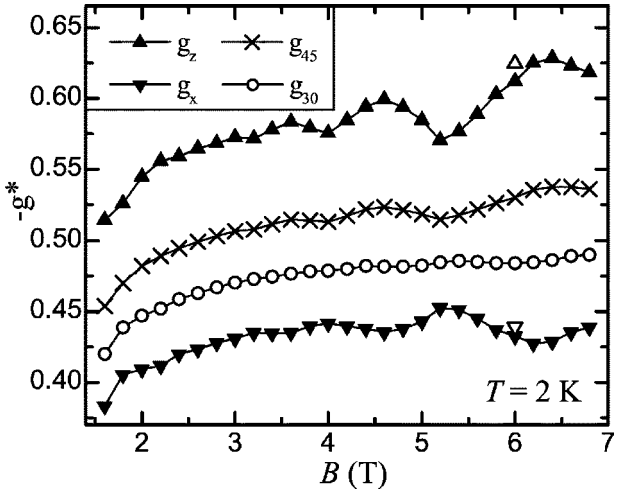


FIG. 2. $g^*$ measured as a function of magnetic field $B$ at 45° (×) and 30° (○) with respect to the growth direction $z$ for sample E and calculated values of $g_z$ (▲) and $g_x$ (▼). The hollow symbols show $g_z$ (△) and $g_x$ (▽) as calculated from the angle-dependent fit shown in Fig. 1(c).

$$|g_\alpha| = \sqrt{g_x^2 \cos^2 \alpha + g_z^2 \sin^2 \alpha}. \qquad (2)$$

The solid line in Fig. 1(c) is a fit from which $g_x=-0.439$ and $g_z=-0.624$. Measurements taken at 30° ($g_{30}$) and 45° ($g_{45}$) as a function of field are used to solve for $g_x$ and $g_z$ in Fig. 2. The oscillations in $g^*$ are more prominent when measured in the 45° reflection geometry, where a larger component of the magnetic field is out of plane. The results of fitting the data in Fig. 1(c) to Eq. (2) are plotted as hollow symbols at $B=6$ T for comparison. We account for the discrepancy with an estimated error in determining $\alpha$ of ±3°. In order to minimize the effect on $\Omega_L$ from the hyperfine interaction with nuclei,[12] a photoelastic modulator was used to polarize the electron spins, as the time-averaged electron spin population

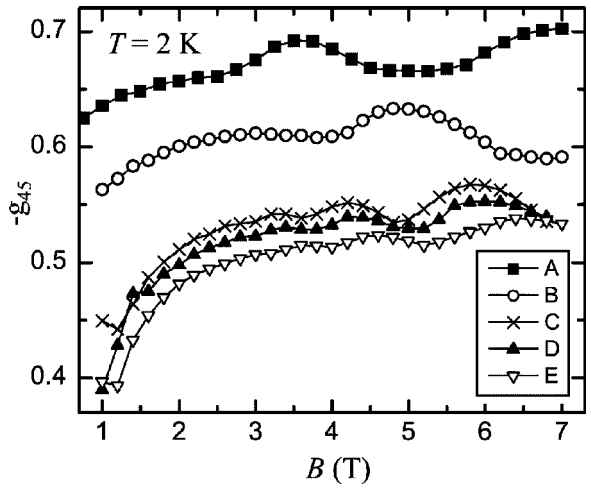


FIG. 3. $g_{45}$ measured in the 45° reflection geometry for samples A (barrier doping density $5\times10^{16}$ cm$^{-3}$), sample B ($1\times10^{17}$ cm$^{-3}$), sample C ($3\times10^{17}$ cm$^{-3}$), sample D ($5\times10^{17}$ cm$^{-3}$), and sample E ($8\times10^{17}$ cm$^{-3}$).

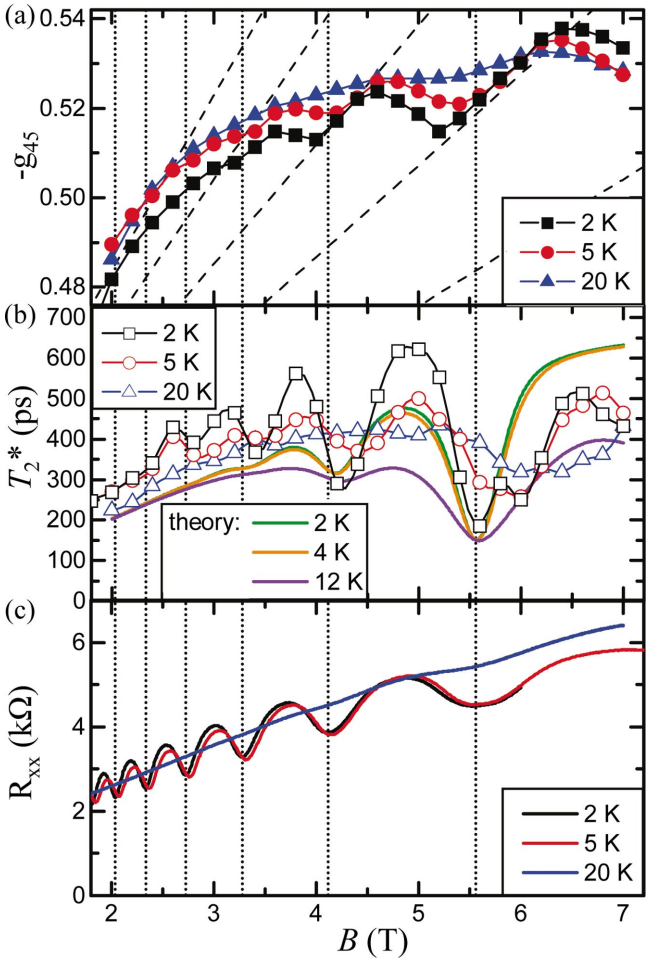


FIG. 4. (Color) (a) $g^*$ measured in the 45° reflection geometry for sample E as a function of $B$ at $T=2$ K, 5 K, and 20 K (symbols). Also plotted (dashed lines) is $g(B,n)=g_0-c\left(n+\frac{1}{2}\right)B$, with $g_0=0.405$ and $c=0.00314$ for $n=4$ to 12. (b) $T_2^*$ measured (symbols) as a function of B at $T=2$ K, 5 K, and 20 K and calculated (lines) from a spin relaxation model at $T=2$ K, 4 K, and 12 K. (c) $R_{xx}$ as a function of $B$ at $T=2$ K, 5 K, and 20 K. Also shown are dotted lines indicating the position of $B_n$ for $n=6$ to 16.

from a waveplate switching between right and left circular polarization should be zero. In addition, measurements are performed at varying laboratory time intervals in order to check that the nuclear spins have a negligible effect on the data. Comparisons of $\Omega_L$ at positive and negative fields show the steady-state nuclear field to be less than 1% of the applied field.

The field dependence of $g^*$ as measured in the 45° reflection geometry ($g_{45}$) for all five samples is plotted in Fig. 3. All samples exhibit the same qualitative behavior, with the magnitude of $g_{45}$ first increasing with the magnetic field and then crossing over to an oscillatory regime at a higher field. As the carrier density is increased from sample A to sample E, the $g$ factor increasingly reflects the value of the bulk GaAs $g$ factor (−0.44), indicating enhanced penetration of the electron wave function into the barriers, while the period of the oscillations seems to decrease, consistent with the decreasing spacing of the Landau levels with the increasing sheet density of the 2DEG.

Similarities between $g^*$ and Shubnikov–de Haas oscillations in the 45° reflection geometry, illustrated with data for sample E at $T=2$ K, 5 K, and 20 K in Fig. 4, indicate that $g^*$ is dependent on the filling factor $\nu$. The vertical dotted lines in Fig. 4 indicate $B_n$ for $n=6$ to 16. Previous measurements of spin precession frequencies in a 2DEG using EDESR established a linear relation between $g^*$ and the Landau-level index $n$:

$$g(B,n)=g_0-c\left(n+\tfrac{1}{2}\right)B, \tag{3}$$

where $g_0$ and $c$ are sample-dependent constants, but $g^*$ could only be measured in regions of field around odd filling factors.[4] Our measurement covers a wider magnetic field range, revealing oscillatory behavior of $g^*$ as a function of $B$ that tracks the behavior of the Shubnikov–de Haas oscillations. We fit our data in regions near full filling to obtain $g_0=0.405$ and $c=0.00314$ for our sample and plot the calculated $g$-factor dependence in Fig. 4(a) for $n=4$ to 12 (dashed lines). The temperature dependence of the TRFR data demonstrates that the amplitude of the oscillations in $g^*$ diminishes as the temperature is increased from 2 to 20 K. Likewise, the Shubnikov–de Haas oscillations, evident in the magnetic field range presented here at 2 and 5 K, are faint below 5 T at 20 K. We observe from power dependences of our measurement that the data presented here are in a regime where the number of optically injected carriers does not change the $g$ factor, indicating a minimal effect of the pump-probe measurement on the Fermi level.

While a dependence in the $g$ factor on Landau-level occupation has been observed previously,[4] oscillatory behavior in $T_2$ has not been reported before. $T_2^*$, as measured in the 45° reflection geometry at 2 K, 5 K, and 20 K, is plotted in Fig. 4(b). From the data, we observe that at low field, $T_2^*$ increases quadratically and at high field, $T_2^*$ exhibits oscillations in magnetic field whose minima correspond to $B_n$. We next discuss a theoretical model which explains the dependence of the spin coherence time on magnetic field. This model calculates the spin relaxation rate $T_2^{-1}$ by considering three contributions: a quadratic fit at low field reflecting the suppression of the D'yakonov-Perel' spin relaxation mechanism,[13] a constant background spin relaxation rate of 1.2 $\text{ns}^{-1}$, and a variance of $g$-factor mechanism, which employs the results of a quantitative calculation based on a generalized $\mathbf{K}\cdot\mathbf{p}$ envelope-function theory solved in a 14-band restricted basis set.[14] In the absence of an applied magnetic field, the D'yakonov-Perel' (DP) spin relaxation rate $T_2^{-1}$ is

$$T_2^{-1}=\Omega^2\tau_o, \tag{4}$$

where $\Omega$ is the precession frequency about the internal DP field and $\tau_o$ is the orbital coherence time. As is consistent with the DP mechanism, the application of an external magnetic field increases the spin coherence time by a factor that is quadratic in applied magnetic field[15]

$$T_2(B)=T_2(0)(1+a^2B^2). \tag{5}$$

A fit to the data taken at 2 K for the magnetic field range 1–2.6 T yields $T_2(0)=57$ ps and $a=0.96$ $\text{T}^{-1}$. This is the reason for the strong dependence of $T_2^*$ with $\alpha$ in Fig. 1(c). The

dotted line in Fig. 1(c) is calculated using Eq. (5) and the values for $T_2^*$ and $a$ obtained above. At large angle, the disagreement may be explained by the contribution from the variance in $g$-factor mechanism to the spin relaxation time. The Elliot-Yafet mechanism is less sensitive to the external magnetic field.[16] Above 3 T, $T_2^*$ exhibits an oscillatory dependence on field that tracks the Shubnikov–de Haas oscillations. These oscillations are related to inhomogeneous dephasing of the spin coherence due to the changing occupation of the Landau levels with magnetic field. If the width of the Landau levels is comparable to the Landau-level spacing, there will be a number of partially occupied Landau levels; this occupation will change with field as the spacing between Landau levels increases. Since electrons in different Landau levels have different spin precession frequencies, the $T_2^*$ that we measure can be dominated by the variance in the $g$-factor destroying the phase coherence of the optically injected spin magnetization. For the variance in the $g$ mechanism, $T_2^{-1} \propto \langle \delta g^2 \rangle \tau_o$, where $\langle \delta g^2 \rangle$ is the variance of $g$. For the calculations shown in Fig. 4(b), the inhomogeneous broadening of the Landau levels is 2.6 meV and $\tau_o = 360$ ps. This orbital coherence time is surprisingly long but may be due to the importance of localized states located energetically between the Landau levels. In addition, the calculations appear to underestimate the oscillation magnitude of $g$ itself.

Another contribution to the oscillatory behavior in $T_2^*$ may be related to the changing density of states at the Fermi level, which would lead to a magnetic field dependence of the scattering time.[17] In our data in Fig. 4(b), however, the minima of $T_2^*$ correspond with minima in $R_{xx}$ and thus the maxima of the conductivity. When the conductivity is largest, the density of states is largest and the scattering time is smallest.[18,19] Thus, from Eq. (4), $T_2^*$ should be at a maximum when the resistance is a minimum from the Ref. 17 model.

The amplitude of the oscillation in the spin coherence time decreases with increasing temperature. As the temperature increases, the width of the Landau levels increases, which causes the features in $g^*$ and $T_2^*$ to become less distinct, both in the measurements and calculations.

In summary, we have measured the electron-spin precession frequencies and spin coherence times as a function of perpendicular magnetic field and observed oscillatory features that indicate a dependence on Landau-level quantization. Measurements were performed on samples of varying doping densities at a variety of temperatures and magnetic field. The effective $g$ factor $g^*$ in semiconductors varies widely for materials as it exhibits a strong dependence on the band-gap energy and spin-orbit coupling; here we have explored the effect of orbital quantization on $g^*$. The spin coherence time also exhibits an oscillatory dependence on Landau-level filling which may be dominated by inhomogeneous dephasing. These oscillations are qualitatively consistent with calculations of $\langle \delta g^2 \rangle$ for this system. The results indicate a possible pathway towards spin manipulation using orbital quantization; electrical control of the carrier density could be used to change the Landau-level filling in a fixed magnetic field with dramatic effects on the $g$ factor and spin coherence time.

We wish to acknowledge the support of DARPA and ARO MURI.

*Electronic address: awsch@physics.ucsb.edu

[1] S. A. Wolf, D. D. Awschalom, R. A. Buhrman, J. M. Daughton, S. von Molnar, M. L. Roukes, A. Y. Chtchelkanova, and D. M. Treger, Science **294**, 1488 (2001).

[2] *Semiconductor Spintronics and Quantum Computation, Nano-Science and Technology*, edited by D. D. Awschalom, N. Samarth, and D. Loss (Springer-Verlag, New York, 2002).

[3] D. Stein, G. Ebert, K. von Klitzing, and G. Weimann, Surf. Sci. **142**, 406 (1984).

[4] M. Dobers, K. von Klitzing, and G. Weimann, Phys. Rev. B **38**, 5453 (1988).

[5] N. Nestle, G. Denninger, M. Vidal, C. Weinzierl, K. Brunner, K. Eberl, and K. von Klitzing, Phys. Rev. B **56**, R4359 (1997).

[6] F. F. Fang and P. J. Stiles, Phys. Rev. **174**, 823 (1968).

[7] G. Bauer and H. Kahlert, Phys. Rev. B **5**, 566 (1972).

[8] S. A. Crooker, D. D. Awschalom, J. J. Baumberg, F. Flack, and N. Samarth, Phys. Rev. B **56**, 7574 (1997).

[9] C. Weisbuch and C. Hermann, Phys. Rev. B **15**, 816 (1977).

[10] J. Konopka, Phys. Lett. **26A**, 29 (1967).

[11] G. Salis, D. D. Awschalom, Y. Ohno, and H. Ohno, Phys. Rev. B **64**, 195304 (2001).

[12] G. Salis, D. T. Fuchs, J. M. Kikkawa, D. D. Awschalom, Y. Ohno, and H. Ohno, Phys. Rev. Lett. **86**, 2677 (2001).

[13] M. I. D'yakonov and V. I. Perel', Zh. Eksp. Teor. Fiz. **60**, 1954 (1971) [Sov. Phys. JETP **33**, 1053 (1971)].

[14] W. H. Lau, J. T. Olesberg, and M. E. Flatté, cond-mat/0406201; Phys. Rev. B (to be published).

[15] *Optical Orientation, Modern Problems in Condensed Matter Science*, edited by F. Meier and B. P. Zachachrenya (North-Holland, Amsterdam, 1984), Vol. 8.

[16] R. Elliott, Phys. Rev. **96**, 266 (1954).

[17] A. A. Burkov and L. Balents, Phys. Rev. B **69**, 245312 (2004).

[18] T. Ando, A. B. Fowler, and F. Stern, Rev. Mod. Phys. **54**, 437 (1982).

[19] T. Ando, J. Phys. Soc. Jpn. **37**, 1233 (1974).